Correction of Diffuse X-Ray Detector Based Background

Axel LANGE, Manfred P. HENTSCHEL, Andreas KUPSCH, Bernd R. MÜLLER
BAM Federal Institute for Materials Research and Testing, 12200 Berlin, Germany

Abstract. A novel approach to strongly suppress artifacts in radiography and computed tomography caused by the effect of diffuse background signals ("backlight") of 2D X-ray detectors is suggested. Depending on the detector geometry the mechanism may be different, either based on the optical scattering of the fluorescent screen materials into optical detection devices or Compton or X-ray fluorescence scattering by the detector components. Consequently, these erroneous intensity portions result in locally different violations of Lambert Beer's law in single projections (radiographs).

When used as input data for computed tomography these violations are directly observed via modulation of the projected mass as a function of the rotation phase and the sample's aspect ratio (dynamics). The magnitude of the diffuse background signal depends on the detector area covered by the projected sample. They are more pronounced the smaller the shaded area and the stronger the total attenuation. Moreover, the local intensity mismatch depends on the attenuation of the sample.

We present very basic reference data measured with multiple metal foils at a synchrotron radiation source. Beam hardening artifacts can be excluded due to the monochromatic radiation. The proposed correction procedure assumes a constant (non-local) scattering mechanism.

Introduction

The rigorous validity of Lambert Beer's law of attenuation is often ignored in qualitative radiology. The emphasis is on the mere perceptibility of the material structure, flaws etc. of interest. The most practical radiographic applications employ polychromatic X-rays. This hampers a quantitative estimation of beam hardening since it requires a case specific calculation taking into account the actual combination of source, sample and detection system and eventually hinders a comparison to tabulated reference values.

Furthermore, scattering effects (arising from refraction, diffraction and incoherent Compton scattering) cause unwanted distortions of intensity. Instead of fundamental corrections contemporary calibration procedures of 2D detectors focus mainly on pixel calibration [1]. For computed tomography (CT) measurements qualitatively proper single projections are inevitable for high reconstruction quality, i.e. the validity of Lambert-Beer's law must be warranted for such simple reasons as the conservation of integral projected mass for all projection angles.

Even the best measuring conditions available (such as parallel and monochromatic synchrotron radiation) do not warrant this invariance. Nevertheless, experimental imponderabilities are reduced to a minimal extent (or can be determined experimentally, at least). Doing so, the causing effect of intensity distortion can be traced back to a diffuse detector based background signal, which obviously causes the violation of the absorption law.

The scope of this study is to demonstrate the experimental findings at the example of rather simple experimental setups and to suggest a first-order approach in order to systematically correct the calculated mismatch of absorption data.

1. Measurements

In a first example the measured phenomenon is on purpose demonstrated by means of a simple CT measurement under well-defined experimental conditions. For a given detection system these conditions refer to the sample (shape, homogeneity) and the radiation (band width, divergence).

An approximately orthorhombic zirconia (ZrO_2) sample (cross section app. 1.18×0.38 mm^2, ρ=6.08 g/cm^3) has been subject to a tomography experiment at the BAM*line* [2] of the synchrotron storage ring BESSY II operated by the Helmholtz Zentrum Berlin (HZB) The sample has been rotated through 180 deg in steps of 0.25 deg (10 s per single projection).

By using a double multilayer monochromator (150×(1.2 nm Si + 1.68 nm W)) the parallel broad band synchrotron radiation is monochromatized to 60 keV (band width 2%, μ_{ZrO2}(60 keV) =17.77 cm^{-1} [3]). A 7 µm $Y_3Al_5O_{12}$:Ce (YAG) scintillator [2] is used to convert X-rays into visible fluorescence light. The visible light is collected by a microscope objective (Rodenstock *TV-Heliflex*, *f* = 50mm, NA= 0.45, 3.6×) and detected by a Princeton Instruments CCD *camera VersArray: 2048B* (2048 × 2048 Pixel) with Nikon *Nikkor 180/2.8 ED* objective. The effective pixel size amounts to 3.72 µm.

Fig.1 (top row) displays a schematic cross section of the sample and a „mass sinogram as measured“. The conversion of measured intensity to „mass“ according to Lambert-Beer’s law follows

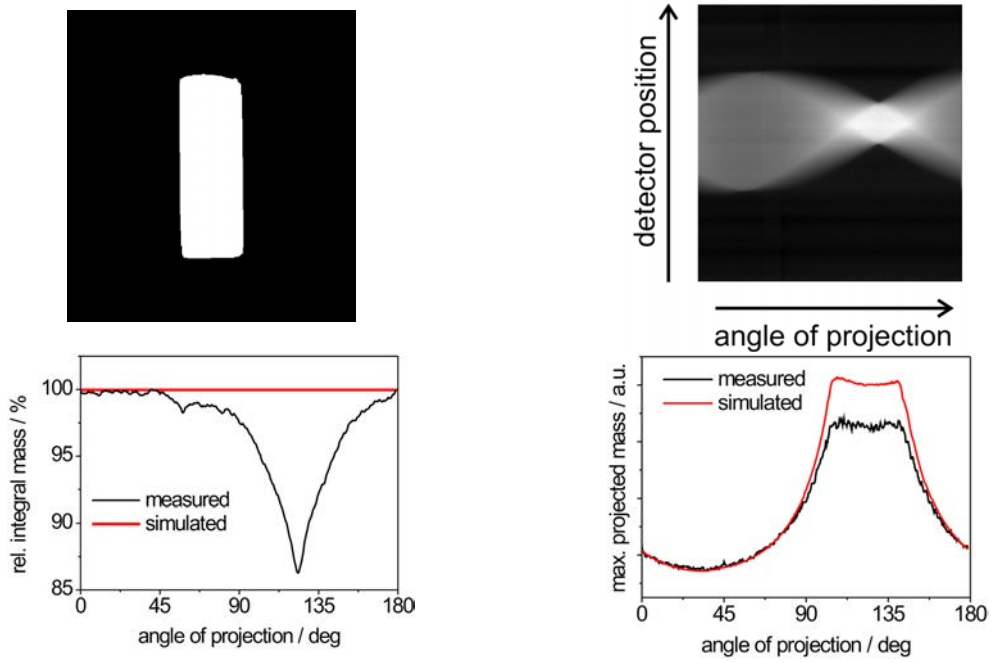

Fig. 1. Representative cross section of the ZrO_2 sample (simulation, top left) and the respective „mass sinogram“ (180 deg measurement, top right). Plotting the integral mass vs. the angle of projection (bottom left) reveals a deviation up to 14% with respect to the required conservation of mass at 120 deg, where the long edge points into the beam direction. This corresponds locally to the deviation of the maximum projected mass (bottom right).

$$(\mu * D)(\mathbf{r}) = \int \mu(\mathbf{r}, z)\mathrm{d}z = \ln\left(I_0(\mathbf{r}) / I(\mathbf{r})\right) . \qquad (1)$$

In the following the term „mass“ is used synonymously for the quantity μ*D which is the product of the attenuation coefficient μ and the transmission chord length $D(z)$. $I(\mathbf{r})$ and $I_0(\mathbf{r})$ denote the intensities of sample and flat field measurements at image position $\mathbf{r}$.
The mass sinogram exhibits two peculiarities:

(i) The integral mass, i.e. integrating each line of the sinogram, is no conserved quantity at all projection angles. It deviates up to 14% from constant (Fig. 1, bottom left).

(ii) Owing to the sample's homogeneity of

$$\mu(\mathbf{r}, z) = \mu_0, \quad \int \mu(\mathbf{r}, z)\mathrm{d}z = \mu_0 * D(\mathbf{r}) \qquad (2)$$

the maximum projected mass must be proportional to maximum transmission chord length. Depending on the projection angle substantial differences are observed. They reach a maximum in the range of the large chord lengths and at small cross sections (Fig. 1, bottom right).

This means that the minimal requirements to CT input data are heavily violated. As a consequence the reconstruction suffers from strong artifacts.

2. Deviations from Lambert-Beer's law - a basic experiment

In order to investigate the observed effect the (measured) absorption behavior of stacked metallic foils is determined. The photon energy applied is 15 keV. The fluorescent screen is made of 50 µm $CdWO_4$ on YAG substrate.

12.5 µm tin foils are chosen. The number N of foils is successively increased from 1 to 8. The attenuation coefficient of tin (Z=50, ρ=7.3 g/cm^3) at 15 keV is μ_{Zn}=34.05 mm^{-1}[3]. This results in an attenuation of exp(-0.425)= exp(-(μ*D)$_0$) per single foil. In order to satisfy equ.(2) the linear dependence of (μ*D)(N)=N*(μ*D)$_0$ is to be expected. This examined as an *integral criterion* derived from the mean values of sample and flat field measurements.

Beyond this a vertical banded background modulation of the primary beam is observed. It originates from the double multilayer monochromator. Since sample and flat field measurements are performed immediately one after the other no temporal changes of the modulation can be neglected. That's why the transmission image $T(\mathbf{r})=I_0(\mathbf{r}) / I(\mathbf{r})$ is examined for cancelled or remaining „multilayer stripes“ as a *local criterion.*

2.1 Full detector coverage

In the first part of the experiment the tin foils were sized larger than the projection of the active detector area. Both the local and integral criterion is fulfilled in good approximation: stripe modulations and local detector irregularities are cancelled in the transmission image (Fig. 2, left). This is proved numerically considering the respective variances σ: σ($I(\mathbf{r})$) ~ 15% clearly exceeds the estimated 3 % to be expected for a mean intensity of 950 counts, i.e. the background modulation rules the variance. In contrast the transmission image exhibits a variance of merely 2.4%.

The linear dependence $(\mu^*D)(N) = N^*(\mu^*D)_0$ is fulfilled, as well (Fig. 2, right). The mean value $(\mu^*D)_0$ is in very good approximation to the tabulated values 0.430(2), μ=34.4 mm^{-1} given above. The deviations of about 1% originate from fluctuations in thickness of the single foils.

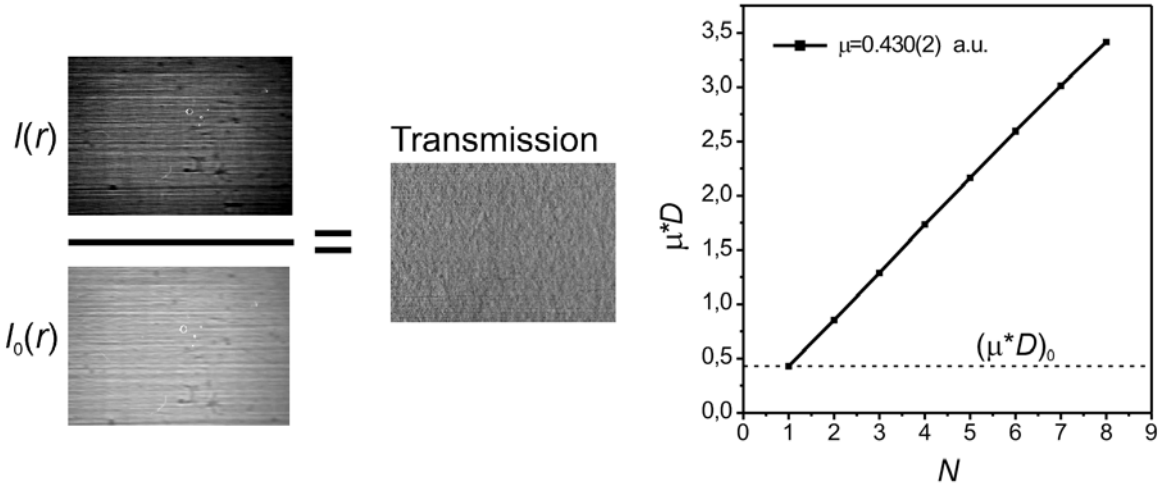

Fig. 2. Left: fully covering the detector area (fluorescent screen) with a homogeneous absorbing material (here: 5×12.5 µm tin) yields a conventionally calculated transmission image (after correction for dark current) free of „multilayer stripes“. Right: The logarithmic integral of the transmission images of gradually stacked foils yields a linear dependence $N^*(\mu^*D)_0$ of the measured attenuation as a function of the number N of tin foils.

2.2 Partial detector coverage

In the second part of the experiment the tin foils were cut into sheets which covered approximately half the detector area.

Fig. 3 illustrates that the application of the conventional Lambert-Beer's law yields insufficient results judging from the local and integral criterion. The transmission image detail (extracted from the covered area) clearly reveals remaining modulations. The plot of

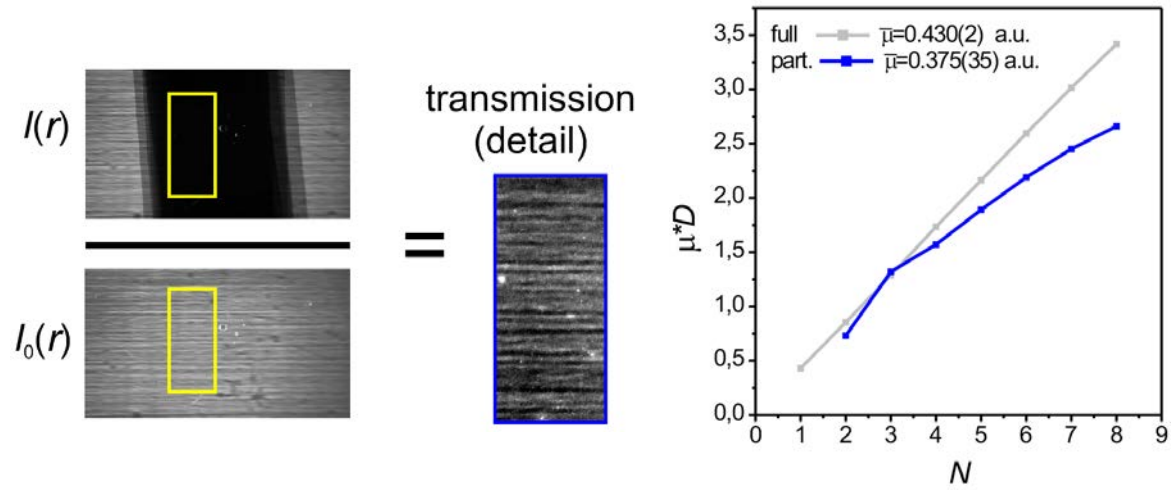

Fig. 3. Left: partially covering the detector area (fluorescent screen) with a homogeneous absorbing material (here: 5×12.5 µm tin) yields a transmission image (of the covered area) which erroneously preserves the „multilayer modulations“. Right: The logarithmic integral of the transmission image details of gradually stacked small foils (blue) exhibits an obvious drift from the linear course as is observed for full coverage (grey, see Fig. 2, right).

μ^*D versus N from the same area is not linear. In particular the difference between the measured (μ^*D) and the true $(\mu^*D)_0$ increases as a function of the absorber thickness (absolute and relative), i.e. the intensity is measured too large.

Fig. 4 compares cumulative cross sections of sample and flat field measurement. While the intensity attenuated by the sample is measured too large the magnified detail of the graphs indicates the reverse effect outside the sample's projected area: the flat field intensity is measured larger (here: app. 2%).

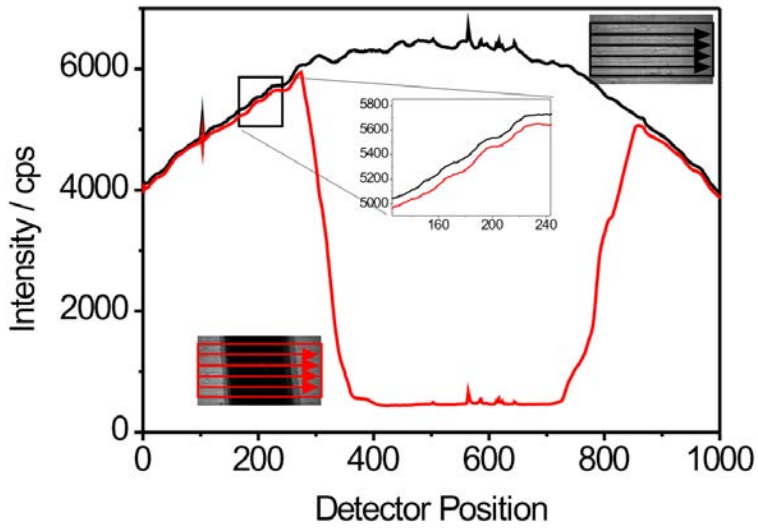

Fig. 4. Cumulative horizontal cross section of sample (red) and flat field measurement (black): outside the sample holds $I_{meas}<I_{flat}$ (ca. 2%, see inset, in contrast to findings in Fig.3 where we observed increased I_{meas} ($>I_{flat}*e^{-N*(\mu^*D)_0}$) inside the sample area.

3. First-order approximation: diffuse detector background - an integral approach

After reporting on the phenomenology of experimental findings we present an explanation and a strategy to correct the obvious mismatches.

The partial levelling of local intensities (i.e. overweighting small and underweighting large intensity) in one and the same sample measurement immediately suggests a partial re-distribution of the locally generated fluorescent intensity to the environment (Fig. 5). This phenomenon is named „*diffuse detector background*" or simply „*backlight*" In a first-order approximation it is assumed to be homogeneous, i.e. the re-distribution of a fraction of local intensity on the entire fluorescent screen (measurement: all detector pixels).

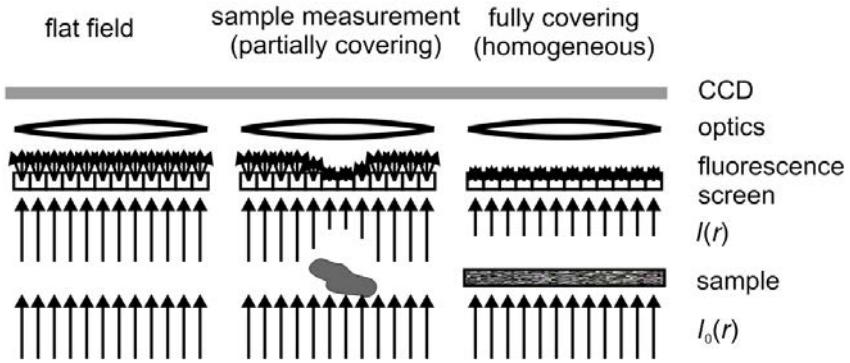

Fig. 5. Principle scheme: The locally generated fluorescence intensity is partially distributed to the environment, thus occurring as a "diffuse detector background" (illustrated at the example of three case scenarios). The length of arrows qualitatively denotes individual intensities.

This fraction α is assumed tobe independent of excitation site and intensity and refers to sample and flat field measurement in the same way. Consequently, both are corrected additively by *one and the same fraction* of their individual mean values:

$$I_{corr}(\mathbf{r}) = I(\mathbf{r}) - \alpha\bar{I}, \quad I_{0,corr}(\mathbf{r}) = I_0(\mathbf{r}) - \alpha\bar{I}_0 \tag{3}$$

The modified intensities of (4) permit the definition of a modified Lambert-Beer's law:

$$(\mu * D)(\mathbf{r}) = \ln\left(\frac{I_{0,corr}(\mathbf{r})}{I_{corr}(\mathbf{r})}\right) = \ln\left(\frac{I_0(\mathbf{r}) - \alpha\bar{I}_0}{I(\mathbf{r}) - \alpha\bar{I}}\right). \tag{4}$$

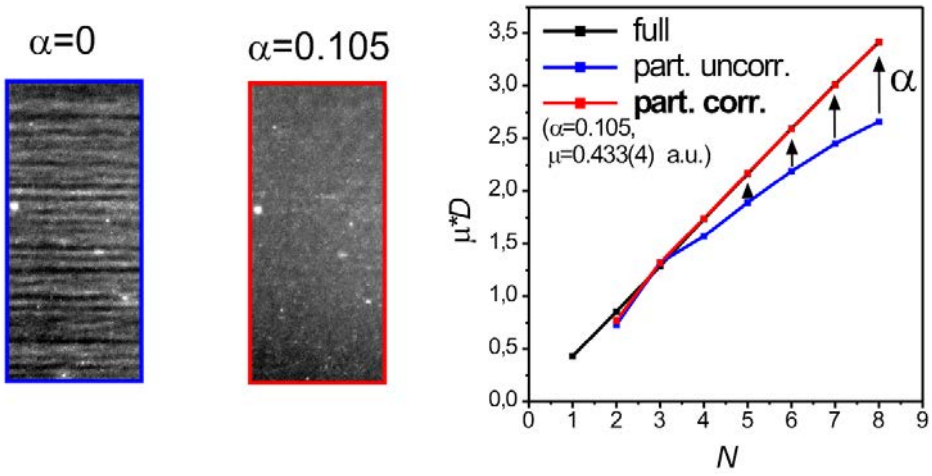

Fig. 6: Results of the suggested integral correction of diffuse detector background. Inserting an optiomized parameter α of 10.5% yields the cancellation of the „multilayer modulations" (left, red frame) from the **transmission** image detail as well as the re-establishment of the integral validity of the (modified) Lambert-Beer's law, illustrated by the red line which follows a linear course (right).

As demonstrated by Fig. 6 the appropriate selection of α in equ. (4) satisfies the required absorption criteria for the local as well as for the integral conditions. The „multilayer modulations" on the uncorrected transmission image (α=0, Fig. 6, left) disappear on the modified image (α=0.105, Fig. 6, center). Moreover the application of a constant α on the uncorrected (blue) plot of μ*D versus N reveals the linear (red) plot which coincides with the plot of the full detector coverage (black, Fig. 6, right). The only required fit condition for finding the optimal α is the linearity requirement min(var((μ*D)/N))) which provides the lowest curvature of the plot. The procedure reveals as well the correct attenuation coefficient μ=34.6 mm^{-1} without further assumptions.

The present approach of a homogeneous background includes obviously the correct validity of the conventional attenuation law in case of full detector coverage as the local intensity modification by the diffuse background contribution is everywhere the same and thus not apparent in the quotient image. Therefore equ.(4) can be applied with any α<1 and α=0 has a physical meaning.

The discussed procedure of integral background correction does not include local variations which may be observed in detail by Fig. 4, which reveals a reduced difference of I_{flat}- I_{meas} further off the sample edge. In relation to the integral intensity deviations the minor variations of the local response are considered to be negligible.

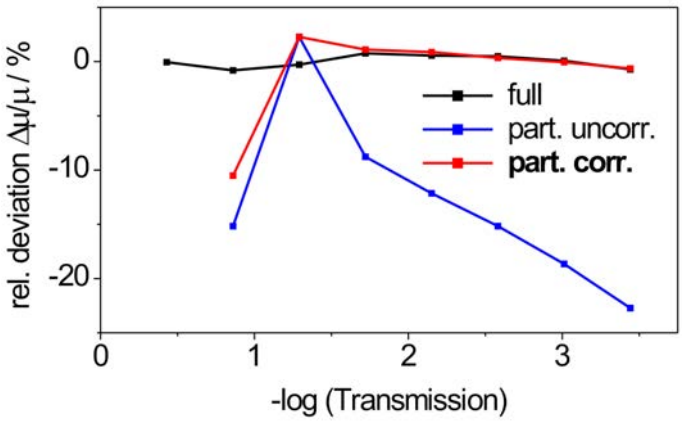

Fig. 7: Relative deviation of the measured attenuation coefficient as a function of μ^*D; "full": full detector coverage by sample, "part uncorr.": partial sample coverage as measured, "part corr." partial sample coverage after correction

4. Summary

The effect of diffuse X-ray detector based background intensity (backlight)

- is characterized by diffusive rearrangement of recorded intensity,
- distorts the measured attenuation coefficient up to some 10% (Fig. 7),
- can be corrected numerically - at least for homogeneous samples,
- decreases with increasing detector coverage,
- increases monotonously with the sample absorption (Fig. 7).

The presented findings permit the quite general advices for all types of X-ray detectors:

- place an aperture behind the fluorescence screen (in order to reduces the detected scattering),
- adapt the primary beam cross section to the sample cross area (reduces the image dynamics),
- alternatively: measure the entire irradiated area (in order to enable numerical correction),
- perform a standard measurement by a well-known reference sample (partial detector coverage)

Although the discussed measurements have been performed by a selected detector system the presented integral correction procedure is largely independent from the detector type. Solely the amount of deficiencies will differ among various systems.

References

[1] C. Schmidgunst, D. Ritter, E. Lang: Calibration model of a dual gain flat panel detector for 2D and 3D x-ray imaging. Med. Phys. **34** (2007) 3649; doi:10.1118/1.2760024

[2] A. Rack, S. Zabler, B.R. Müller, H. Riesemeier, G. Weidemann, A. Lange, J. Goebbels, M.P. Hentschel, W. Görner: High resolution synchrotron-based radiography and tomography using hard X-rays at the BAMline (BESSY II). Nuclear Instruments and Methods in Physics Research **A 586** (2008) 327–344.

[3] data base: http://physics.nist.gov/PhysRefData/XrayMassCoef/